

Phosphatidylinositol 4-kinase is required for endosomal trafficking and degradation of the EGF receptor

Shane Minogue^{1,*}, Mark G. Waugh¹, Maria Antonietta De Matteis², David J. Stephens³, Fedor Berditchevski⁴ and J. Justin Hsuan¹

¹Centre for Molecular Cell Biology, Department of Medicine, Royal Free and University College Medical School, University College London, Rowland Hill Street, London, NW3 2PF, UK

²Department of Cell Biology and Oncology, Consorzio Mario Negri Sud, Via Nazionale, 66030 Santa Maria Imbaro (Chieti), Italy

³Department of Biochemistry, University of Bristol, School of Medical Sciences, University Walk, Bristol, BS8 1TD, UK

⁴CRUK Institute for Cancer Studies, University of Birmingham, Edgbaston, Birmingham, B15 2TA, UK

*Author for correspondence (e-mail: s.minogue@medsch.ucl.ac.uk)

Accepted 20 October 2005

Journal of Cell Science 119, 571-580 Published by The Company of Biologists 2006

doi:10.1242/jcs.02752

Summary

The type II alpha isoform of phosphatidylinositol 4-kinase has recently been shown to function in the recruitment of adaptor protein-1 complexes to the trans-Golgi network. Here we show that phosphatidylinositol 4-kinase II α is also a component of highly dynamic membranes of the endosomal system where it colocalises with protein markers of the late endosome and with endocytosed epidermal growth factor. When phosphatidylinositol 4-kinase II α activity was inhibited *in vivo* using the monoclonal antibody 4C5G or by depression of endogenous phosphatidylinositol 4-kinase II α protein levels using RNA interference, ligand-bound epidermal growth factor receptor failed to traffic to late endosomes and instead accumulated in vesicles in a sub-plasma membrane

compartment. Furthermore, lysosomal degradation of activated epidermal growth factor receptor was dramatically impaired in small inhibitory RNA-treated cells. We demonstrate that phosphatidylinositol 4-kinase II α is necessary for the correct endocytic traffic and downregulation of activated epidermal growth factor receptor.

Supplementary material available online at
<http://jcs.biologists.org/cgi/content/full/119/3/571/DC1>

Key words: Type II phosphatidylinositol 4-kinase, Endocytosis, Degradation, Epidermal growth factor

Introduction

Phosphoinositide (PI) lipids play crucial roles in membrane trafficking by directly altering the physical properties of membranes and by mediating the interaction of proteins containing PI-binding domains (Gruenberg, 2003; Cullen et al., 2001). The 4'-phosphorylated phosphoinositides, phosphatidylinositol 4-phosphate, 4,5-bisphosphate and 3,4,5-trisphosphate [PtdIns(4)P, PtdIns(4,5)P₂ and PtdIns(3,4,5)P₃, respectively] are all, directly or indirectly, the products of Phosphatidylinositol 4-kinase (PtdIns4K) activity and have established roles in membrane traffic. The mammalian PtdIns4Ks belong to two families, type II and type III, both of which have been implicated in multiple membrane-trafficking events. For example, the wortmannin-sensitive PtdIns4KIII β undergoes Arf-dependent recruitment to the Golgi complex (Godi et al., 1999). PtdIns4KII α functions at the trans-Golgi Network (TGN) where it synthesises PtdIns(4)P required to recruit the adaptor protein AP1 from the cytosol (Wang et al., 2003). The same isoform has also been found associated with synaptic vesicles (Guo et al., 2003). In addition to the Golgi complex, PtdIns4KII α and PtdIns4KII β both localise to endosomal membranes containing internalised transferrin and

angiotensin (Balla et al., 2002) and EEA1 (Balla et al., 2002; Waugh et al., 2003a).

Despite the many recognised functions for PtdIns4K isoforms at the Golgi, the role of PtdIns4KIIs in endosomal traffic is currently unclear. Indeed, early reports localising overexpressed recombinant PtdIns4KIIs to endosomal compartments (Balla et al., 2002) have been thrown into doubt (Wang et al., 2003; Wei et al., 2002). On the other hand, we and others have previously noted an agonist-dependent association of PtdIns4KII activity with the EGFR (Cochet et al., 1991; Kauffmann-Zeh et al., 1994), which may in fact be due to the detection of an endocytic event.

The EGFR, as well as being a significant human oncogene (Hsuan, 1993; Roskoski, 2004), is a model system for the study of receptor-mediated endocytosis. This process is known to be dependent on PtdIns(4,5)P₂ for the recruitment of complexes containing clathrin, AP2 and epsin 1 (Ford et al., 2002) and the GTPase dynamin, which is responsible for the fission of clathrin-coated vesicles (CCVs) from the plasma membrane (Oh et al., 1998). Following internalisation, vesicles bearing receptor-ligand complexes are delivered to the tubular-vesicular early endosome. Then after cargo sorting and detaching from early endosomes, endosomal carrier vesicles

are transported via microtubules to the late endosome (Aniento et al., 1993). Late endosomes are characterised by the presence of markers such as the proteins lamp-1 (lgp 120) and CD63, the lipid lysobisphosphatidic acid (LBPA) and by the accumulation of ligands such as EGF at late time points (Felder et al., 1990; Gruenberg and Stenmark, 2004). Late endosomes

are normally located close to the nucleus and concentrated around the microtubule-organising centre in a juxta-Golgi position. In the case of the EGFR, ligand remains bound and signalling from the complex remains active until receptors can be sequestered in multivesicular bodies for subsequent degradation in the lysosome (Futter et al., 1996). Therefore endosomal trafficking of the EGFR plays a key role in the downregulation of activated receptors (Katzmann et al., 2002).

In this study we have characterised the distribution of GFP-tagged PtdIns4KII α in live cells and examined the function of the protein in the endocytosis and degradation of the EGFR-EGF complex by inhibition of endogenous PtdIns4KII α . Our results suggest a key role for PtdIns4KII α in endocytic trafficking and in the downregulation of EGF signalling.

Results

The dynamic subcellular organisation of PtdIns4KII α

Human HT1080 fibrosarcoma cells stably expressing human PtdIns4KII α as an N-terminal GFP-fusion protein were examined by laser-scanning confocal microscopy. In both live and fixed samples, GFP-PtdIns4KII α was found to localise predominantly to relatively large (0.8-1.6 μ m diameter) juxtanuclear structures concentrated in the Golgi region that resemble late endosomes (Fig. 1A). Lesser amounts of GFP-PtdIns4KII α were also observed at the plasma membrane, on small vesicles (0.2-0.6 μ m diameter) and tubular-vesicular structures throughout the cell body (Fig. 1B). In addition, large (0.9-2.9 μ m diameter) structures were observed which were morphologically similar to multivesicular bodies (Fig. 1C). Interestingly, in time-lapse experiments, these large structures were highly dynamic with PtdIns4KII α -containing vesicles and

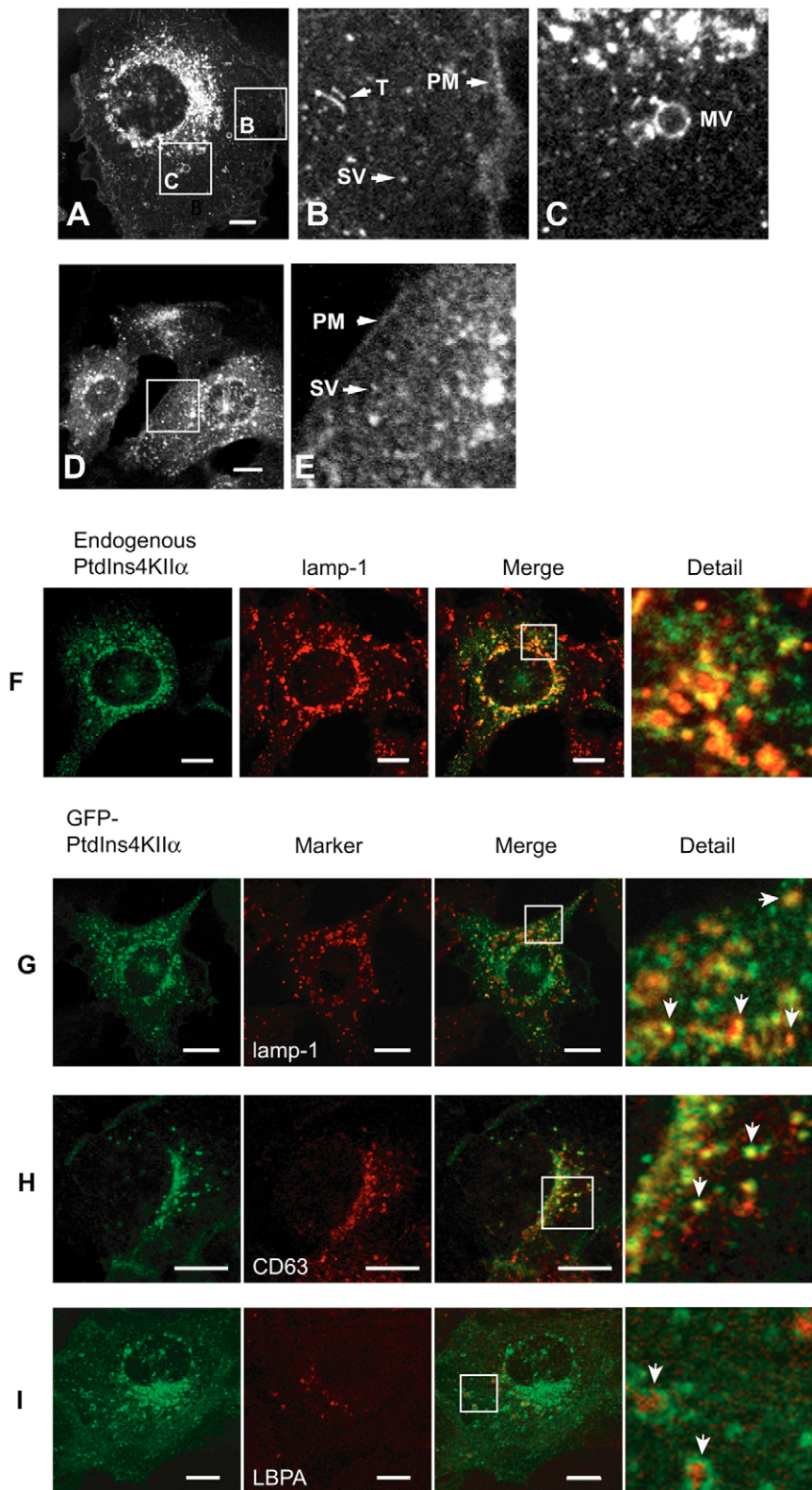


Fig. 1. The subcellular distribution of PtdIns4KII α in HT1080 cells. (A) Live cells expressing GFP-PtdIns4KII α were imaged by confocal laser-scanning microscopy. (B) Detail of plasma membrane (PM), small cytoplasmic vesicles (SV) and tubules (T). (C) Detail of the juxta-nuclear region showing multivesicular body (MVB)-like structures (MV). (D) Endogenous PtdIns4KII α in fixed HT1080 cells and (E) detail. (F) Cells co-immunostained for endogenous PtdIns4KII α and lamp-1. Staining for (G) GFP-PtdIns4KII α and lamp-1, (H) CD63 and (I) LBPA. Arrows in G,H indicate colocalisation of GFP-PtdIns4KII α and marker in punctate structures. Arrows in I indicate the localisation of GFP-PtdIns4KII α to the boundary membrane of MVB-like structures. All zoom boxes are 20 μ m square. Bars, 10 μ m.

tubules apparently fusing with their limiting membranes (supplementary material Movie 1 and Fig. 2E). In order to demonstrate that these were indeed multivesicular bodies, we immunostained the same cells for the late-endosome-specific lipid LBPA using monoclonal antibody 6C4 (Kobayashi et al., 1998). These experiments revealed that LBPA-containing endosomes were frequently observed surrounded by GFP-PtdIns4KII α -rich membranes (Fig. 1I).

We confirmed that the late endosomal localisation of GFP-PtdIns4KII α was not due to partial degradation of the fusion protein in late endosomes by colocalisation of endogenous PtdIns4KII α with lamp-1 (Fig. 1F) using antisera specific for the alpha isoform (supplementary material Fig. S1). It has been reported that overexpression can lead to mislocalisation of PtdIns4KII α and disruption of the Golgi apparatus (Wang et al., 2003). In this study, low levels of overexpression were achieved by using stably transfected cells. Endogenous PtdIns4KII α showed a similar distribution to the GFP-PtdIns4KII α when untransfected HT1080 cells were immunostained with anti-PtdIns4KII α antibodies (Fig. 1D,E) and a similar colocalisation was observed when cells were co-immunostained with PtdIns4KII α and lamp-1 antibodies (Fig. 1F). Western blotting of GFP-PtdIns4KII α HT1080 cell lysates with PtdIns4KII α -specific antibodies (Waugh et al., 2003a) indicated that levels of ectopic expression were similar to those of endogenous protein and furthermore, when control and stably transfected cells were fractionated on sucrose density gradients both showed an identical distribution of endogenous protein, GFP-PtdIns4KII α protein and activity (data not shown). In addition, our GFP-PtdIns4KII α HT1080 cell line did not exhibit any disruption of the Golgi complex or mislocalisation of Golgi markers (data not shown).

Because of the apparently complex pattern of subcellular distribution of GFP-PtdIns4KII α , we sought to define this further using immunocytochemistry. Although we were unable to find an endosomal marker protein showing complete colocalisation with PtdIns4KII α (Fig. 1G,H,I), we and others found colocalisation with markers of endosomal membranes including EEA1, transferrin and internalised angiotensin in Cos-7 cells (Balla et al., 2002; Waugh et al., 2003a). Colocalisation of GFP-PtdIns4KII α and EEA1 and internalised

transferrin was also observed in the HT1080 cells used in this study (supplementary material Fig. S2). The late-endosomal markers lamp-1 and CD63 showed extensive colocalisation on discrete punctae which was particularly evident in the perinuclear region (Fig. 1G,I). Time-lapse imaging of GFP-PtdIns4KII α HT1080 cells revealed numerous small vesicles (0.2–0.5 μ m) moving rapidly at rates of 0.8–1.2 μ m/second (Fig. 2C,D and supplementary material Movie 1). The movement of these vesicles was often discontinuous and they were frequently observed changing direction and fusing with other membrane structures including late endosomes (supplementary material Movie 1).

Given the highly dynamic nature of GFP-PtdIns4KII α in time-lapse experiments and the observed localisation to endosomal membranes in fixed cells, we hypothesised that PtdIns4KII α might be (1) trafficked through the endosomal pathway and (2) that PtdIns4KII activity might be necessary for the motility of the vesicles observed in Movie 1 in supplementary material and in Fig. 2. Despite reports of EGF-stimulated PtdIns4KII activity associated with the EGF receptor (Cochet et al., 1991; Kauffmann-Zeh et al., 1994), we observed only small amounts of PtdIns4KII α at the plasma membrane and we did not observe recruitment of GFP-PtdIns4KII α to the plasma membrane upon stimulation with EGF (Figs 3 and 4). However, the previously observed association between activated EGF receptors and PtdIns4KII activity may be due to EGF-dependent colocalisation in an endosomal compartment.

Epidermal growth factor is trafficked to endosomal structures containing GFP-PtdIns4KII α

We used the fluorescent ligand Rh-EGF to define membranes of the endosomal system: by establishing the time course for Rh-EGF internalisation in HT1080 cells (Fig. 3A), we were able to follow Rh-EGF fluorescence through early and late endosomal compartments in pulse-chase time-course experiments. Serum-starved HT1080 GFP-PtdIns4KII α cells were treated with a 100 ng/ml pulse of Rh-EGF for 120 seconds followed by unlabelled EGF for a further 900 seconds. Cells were fixed at 0, 120, 300, 600, 900 and 1200 seconds and examined by confocal laser-scanning microscopy (Fig. 3A). In

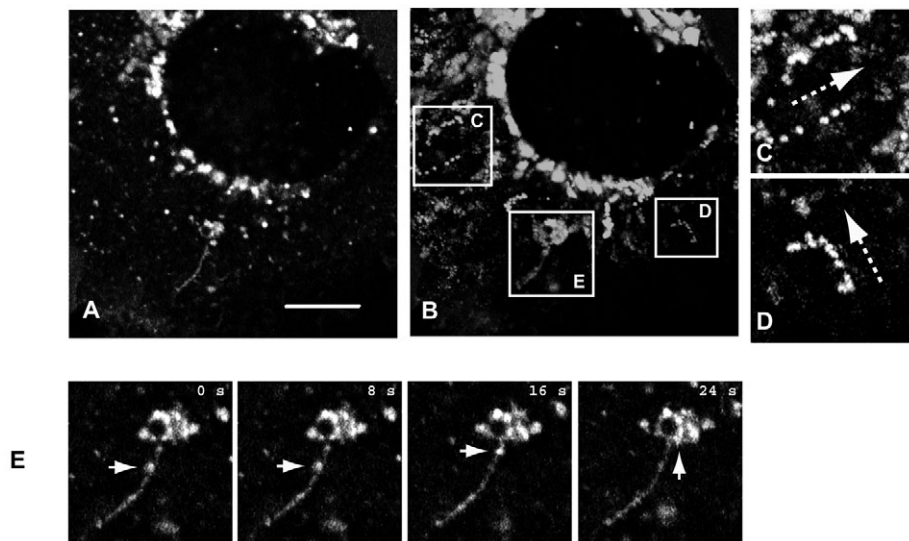


Fig. 2. PtdIns4KII α is a component of highly dynamic membranes. (A) A confocal image of a live GFP-PtdIns4KII α -expressing HT1080 cell. (B) Frames from a time-series experiment were projected in the Z-axis to reveal the paths of moving vesicles. These paths and the direction of movement (arrows) are detailed in C and D. (E) Frames from the same cell showing the progress of a vesicle (arrows) along a tubule toward a multivesicular body (also see supplementary material Movie 1). Bar, 10 μ m.

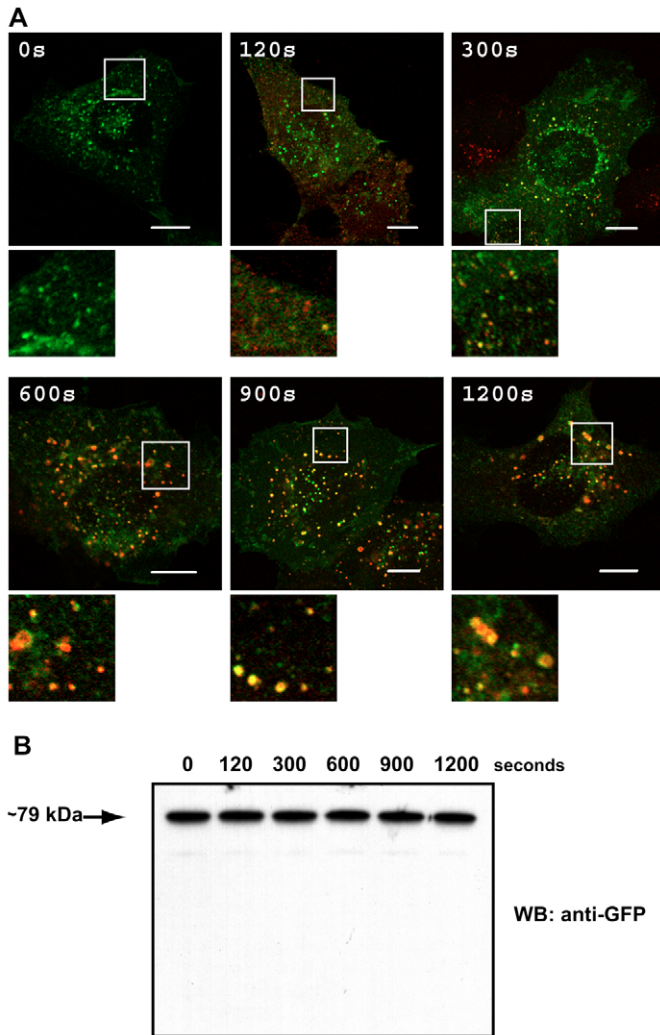


Fig. 3. GFP-PtdIns4KII α colocalises with endocytosed Rh-EGF. (A) Time course of Rh-EGF internalisation in HT1080 GFP-PtdIns4KII α cells. Detail from each time point is shown in the zoom boxes (10 μ m square). (B) Anti-GFP western analysis of total cell lysates from HT1080 GFP-PtdIns4KII α cells stimulated with EGF for the times shown was also performed to rule out the possibility that the endosomal localisation could be due to degradation of the fusion protein. Bars, 10 μ m.

order to rule out the possibility that partial degradation of the GFP-PtdIns4KII α was responsible for the endosomal signal, we analysed cell lysates from each time point with anti-GFP to show that the fusion protein remained intact throughout the time course (Fig. 3B). At later time points, Rh-EGF and GFP-PtdIns4KII α were found to colocalise in large (mean diameter \pm s.e.m. of 0.86 ± 0.26 μ m) juxtanuclear structures some of which were clearly clusters of vesicles. As with live cells, three kinds of structure could be observed: small (0.36 ± 0.18 μ m) vesicles that were generally distributed throughout the cytoplasm, larger roughly spherical or irregularly-shaped structures (0.94 ± 0.28 μ m) with a perinuclear and juxta-Golgi location, and large multivesicular structures (~ 1 μ m) in which GFP-PtdIns4KII α was generally restricted to the boundary membrane (Fig. 1C,D). We also performed time-lapse

experiments on Rh-EGF-stimulated HT1080 GFP-PtdIns4KII α cells (Fig. 4 and supplementary material Movie 2). Again, the bulk of the GFP-PtdIns4KII α was not observed to colocalise with Rh-EGF. However, small, highly mobile (0.22–0.40 μ m, mean velocity 0.6 μ m/second) vesicles containing Rh-EGF and GFP-PtdIns4KII α were observed (Fig. 4 and supplementary material Movie 2).

Effects of PtdIns4KII inhibition on vesicle motility

Given that PtdIns4KII α is highly dynamic in time-lapse experiments and colocalises with EGF in endosomal compartments we hypothesised that PtdIns4KII α activity might be necessary for the endocytosis of EGF-EGFR complexes. In order to test this we employed the PtdIns4K inhibitor phenylarsine oxide (PAO) (Wiedemann et al., 1996), which inhibits both recombinant type II and type III isoforms *in vitro* (Balla et al., 2002). In time-lapse studies using live HT1080 GFP-PtdIns4KII α cells treated with 100 μ M PAO, we found that mobility of the smallest vesicles was dramatically inhibited because no vesicle movement was observed in any cell examined. However, vehicle alone (DMSO, 0.01%) did not impair vesicle movement (results not shown).

PtdIns4KII α is necessary for the traffic of EGFR to late endosomal compartments

We repeated both the fixed time course and live-cell time-lapse experiments using HT1080 cells expressing the kinase dead mutant GFP-PtdIns4KII α (K152A). In both experiments, results were indistinguishable from the HT1080 GFP-PtdIns4KII α (wild-type) cells (not shown). This observation is consistent with reports that kinase-inactive PtdIns4KII mutants do not appear to act in a dominant-negative manner when moderately overexpressed (Balla et al., 2002; Wang et al., 2003) (our unpublished observations). We therefore sought to inhibit endogenous PtdIns4KII activity using the inhibitory mAb 4C5G. This antibody was raised to a partially pure fraction of bovine PtdIns4KII α and has been shown to specifically inhibit type II PtdIns4K activity (Endemann et al., 1991). Although this monoclonal antibody inhibits recombinant human PtdIns4KII α *in vitro* (Minogue et al., 2001), its effects on beta activity are as yet unknown. In many cell lines, including those used here, PtdIns4KII α is by far the more prevalent activity (Waugh et al., 2003b) and we were unable to detect sufficient amounts of PtdIns4KII β to assess the effects of 4C5G against this isoform. Therefore we cannot reliably state that 4C5G is PtdIns4KII α -specific. Consequently, we used this antibody as a general inhibitor of PtdIns4KII activity. To this end, HT1080 cells were transfected with 4C5G using the Chariot protein transfection system. Mock (mAb 9E10)-transfected cells endocytosed Rh-EGF-EGFR complexes in a time course and manner indistinguishable from those in the previous experiment (compare Fig. 5A and Fig. 3). However in cells transfected with mAb 4C5G, Rh-EGF failed to traffic to large vesicles in the juxtanuclear region to the same extent as the control cells (Fig. 5A,B). Instead Rh-EGF was observed in smaller vesicles scattered throughout the cytoplasm and clustered beneath the plasma membrane. These phenomena were particularly apparent at time points greater than 600 seconds.

We then used siRNA transfection to specifically depress levels of PtdIns4KII α protein. HT1080 cells were either

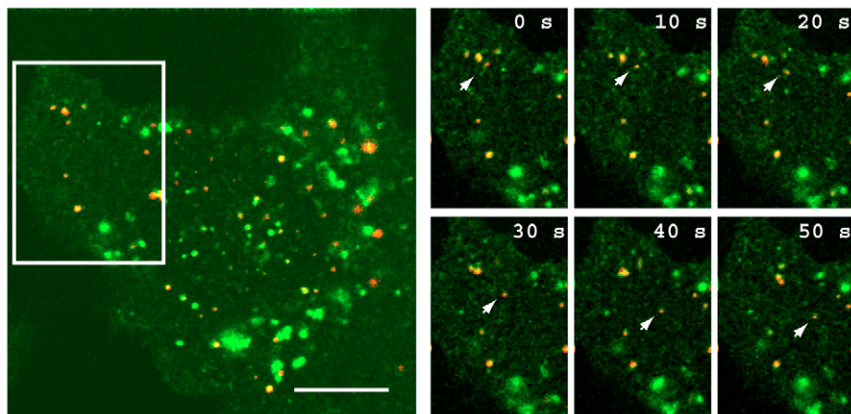


Fig. 4. Internalised EGF is trafficked in rapidly moving PtdIns4KII α -containing vesicles. Time-lapse images were obtained from live HT1080 GFP-PtdIns4KII α cells that had been serum-starved and stimulated with Rh-EGF for 120 seconds. Frames from the boxed region show the movement of a single vesicle marked with an arrow. Also see supplementary material Movie 2. Bar, 10 μ m.

transfected without siRNA oligonucleotide (mock), with siRNA targeting lamin or with one of two 21-mer duplex oligonucleotides targeting PtdIns4KII α (named oligo-1 and oligo-2, respectively). Western blotting of total cell lysates from transfected HT1080 cells showed that levels of PtdIns4KII α and PtdIns4KII β were unaffected whereas oligo-1 and oligo-2 transfected cells showed significant reductions in levels of PtdIns4KII α without affecting the closely related PtdIns4KII β isoform (Fig. 6A). Since oligo-2 was judged to be less effective in reducing levels of PtdIns4KII α , and the lamin siRNA control had no effect, we continued using only oligo-1 siRNA and the mock control for transfection, however the following results were validated quantitatively using all four conditions (see supplementary material Fig. S3).

Similar phenomena to that in the 4C5G experiments were observed in cells in which PtdIns4KII α expression had been reduced to below detectable levels using siRNA oligo-1 (Fig. 6A), instead of being rapidly trafficked to juxtannuclear late endosomes, Rh-EGF-EGFR complexes accumulated in small vesicles (0.2-0.6 μ m) in a sub-plasma-membrane region (Fig. 6C,D). In mock-transfected cells, large juxtannuclear late

endosomal vesicles accumulated at the expense of the sub-plasma membrane vesicles which were virtually absent by 300 seconds (Fig. 6B). By contrast, cells depleted of PtdIns4KII α retained this phenotype throughout the 1200 second time course and furthermore, these cells exhibited a markedly disorganised distribution of Rh-EGF fluorescence in which vesicles remained scattered throughout the cytoplasm (Fig. 6C).

Z-series data were analysed from both the 4C5G and RNAi experiments. We noted that the average diameter of Rh-EGF-labelled vesicles was 27.3% smaller in 4C5G-treated and 46% smaller in siRNA-treated cells compared with their respective controls at the 1200 second time points (Fig. 7A,D). In addition, although control cells continued to accumulate Rh-EGF-EGFR in vesicles which increased in diameter as they matured to late endosomes, the increase in mean diameter of vesicles in 4C5G-treated or PtdIns4KII α -siRNA-treated cells was markedly retarded. This trend is illustrated in Fig. 7B,E which show the percentage of cells with scattered cytoplasmic vesicles. Like GFP-PtdIns4KII α -HT1080 cells, mock-transfected cells readily accumulate Rh-EGF-EGFR in

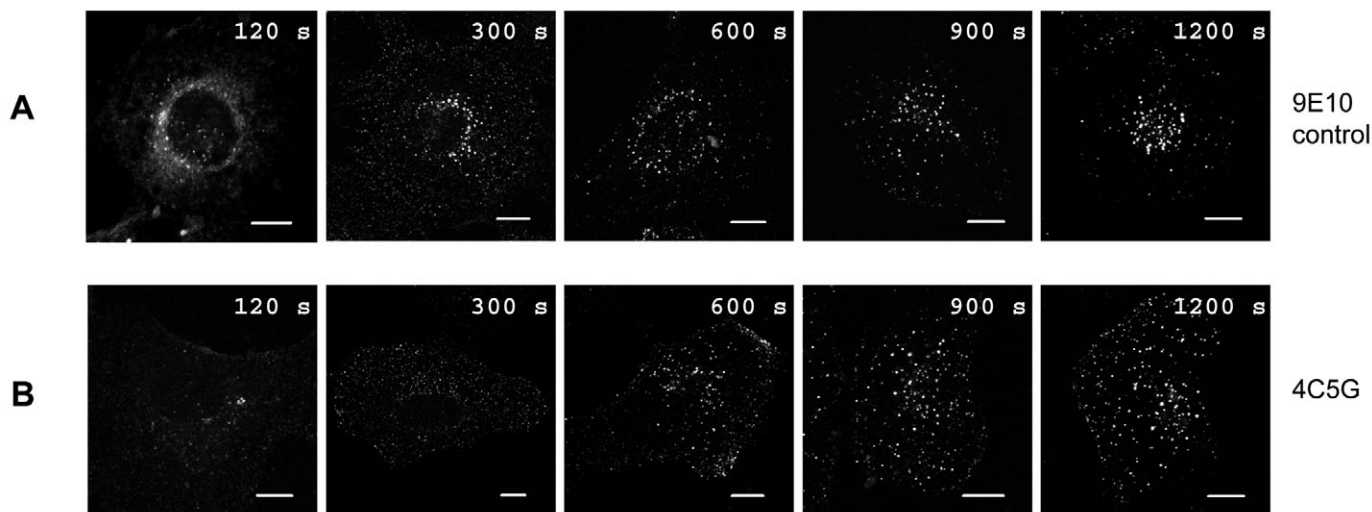


Fig. 5. Inhibition of endogenous PtdIns4KII activity results in abnormal trafficking of internalised EGF. HT1080 cells were transfected with control monoclonal antibody 9E10 (A) or 4C5G (B) and, after serum starvation, stimulated with Rh-EGF then fixed at the time points indicated. All images are extended focus views representing 12 confocal sections collected 0.12 μ m apart. Bars, 10 μ m.

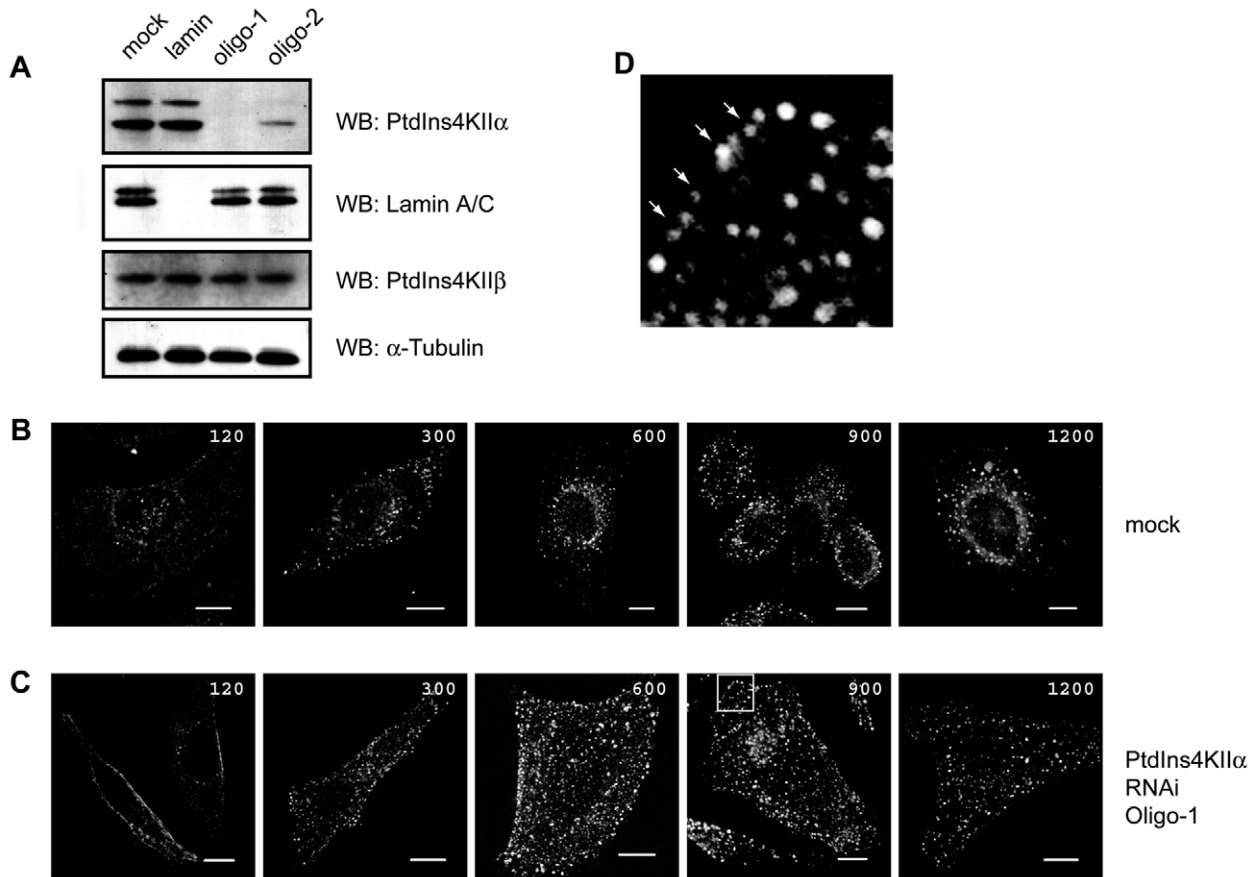


Fig. 6. Inhibition of PtdIns4KII α mRNA expression results in the abnormal trafficking of internalised EGF. (A) siRNA with two independent duplex oligonucleotides (oligo-1 and oligo-2) effectively depletes HT1080 cells of PtdIns4KII α but not the closely related isoform PtdIns4KII β (the doublet in the PtdIns4KII α blot is frequently observed). A time course of Rh-EGF internalisation in HT1080 cells in mock (B) or PtdIns4KII α siRNA (C) transfected cells. (D) Detail of the boxed sub-plasma membrane region from the 900 seconds time point from C. Arrows indicate the retention of Rh-EGF in sub-plasma membrane punctae. All images are extended focus views representing 12 confocal sections collected 0.12 μ m apart. Bars, 10 μ m.

juxtannuclear late endosomes, such that at the 1200 seconds time point no cells contained scattered vesicles in 9E10 and mock-RNAi controls (Fig. 7B,E). By contrast, cells transfected with 4C5G retained this scattered phenotype in 92.5% (\pm 3.8%) of cells or 98% (\pm 2.0%) of cells (PtdIns4KII α siRNA) at the 1200 seconds time points respectively. Accumulation of sub-plasma-membrane vesicles was observed at the same time points in 96% (\pm 4%) of 4C5G-treated cells and 93% (\pm 3.7%) of alpha RNAi cells and compared with 7.5% (\pm 3.8%) and 0% for 9E10 and mock RNAi controls, respectively (Fig. 7C,F).

RNAi treatment impairs degradation of the EGFR

We reasoned that impairing the traffic of EGFR to late endosomes should affect the rate of traffic to downstream degradative compartments. To address this question we examined the effect of PtdIns4KII α RNAi on the degradation of EGFR. For this experiment we used HeLa cells, which typically gave 90% knockdown of PtdIns4KII α protein after 72 hours, thus making them ideal for biochemical experiments. HeLa cells were transfected with no oligonucleotide (mock), with siRNA to lamin and with two independent siRNA targeting PtdIns4KII α , oligo-1 and oligo-2. The cells were subsequently serum-starved and stimulated with unlabelled

EGF for 0, 0.5, 1 and 2 hours in the presence of 10 μ g/ml cycloheximide. When degradation of the EGFR was monitored by western blotting it was found that oligo-1 and oligo-2 siRNA-treated cells retained a significant amount of intact EGFR over the whole time course when compared with mock and lamin siRNA-transfected cells (Fig. 8A,B).

Discussion

In this study we have extensively characterised the dynamics of PtdIns4KII α in live cells using time-lapse imaging and have found that PtdIns4KII α is distributed between the plasma membrane, small highly mobile vesicles, large juxtannuclear late endosomes and the limiting membranes of multivesicular bodies. Further evidence that these were late endosomes was provided by colocalisation with lamp-1, CD63, LBPA and with internalised Rh-EGF at late time points (Fig. 1F,G,H and Fig. 3). The heterogeneous vesicular distribution of PtdIns4KII α suggested that this protein is either being trafficked or has itself a function in intracellular traffic. Indeed, prior to the identification of the PtdIns4KII cDNAs, PtdIns4KII activity was known to be present in purified membranes derived from the endo-lysosomal system (Collins and Wells, 1983). More recently, several studies have been published describing the

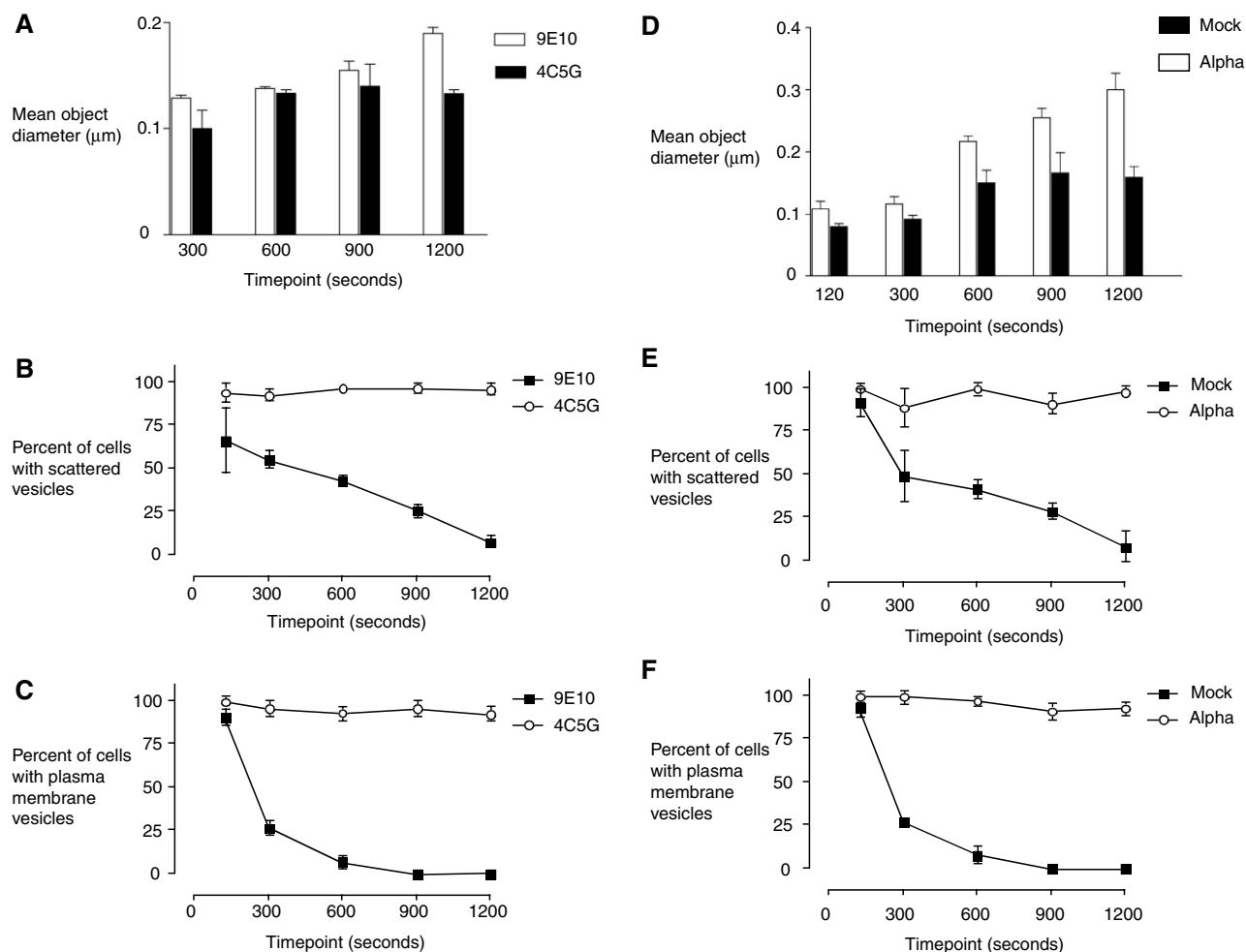


Fig. 7. The effects of in vivo PtdIns4KII inhibition on the endosomal distribution of internalised EGF. Z-series data from time course experiments were reconstructed in three dimensions and the mean diameter of Rh-EGF-labelled punctae measured as described in the Materials and Methods. Punctae were analysed in single cells (300–800 objects per cell) from at least three cells from three independent time course experiments (i.e. 2.7×10^3 – 7.2×10^3 objects per time point). (A) Analysis of mean vesicle diameter (\pm s.e.m.) in 9E10 and 4C5G-transfected cells. The same cells were also scored for scattered punctae (B) and sub-plasma membrane vesicle clusters (C). (D) Analysis of mean vesicle diameter (\pm s.e.m.) in mock-transfected and PtdIns4KII α siRNA-transfected cells. Rh-EGF treated cells were also manually scored for the presence of scattered punctae (E) and the persistence of small vesicles clustered beneath the plasma membrane (F). For B,C and E,F, a minimum of 63 cells per time point were scored from three independent experiments.

subcellular localisation of PtdIns4KIIIs in the Golgi complex (Wang et al., 2003; Wei et al., 2002) and in early endosomes (Balla et al., 2002; Waugh et al., 2003a). Of particular relevance to the present study is work from the Balla laboratory demonstrating that GFP-PtdIns4KII α colocalises with the internalised receptor ligand angiotensin and that transferrin uptake was markedly inhibited in Cos-7 cells overexpressing a kinase-inactive PtdIns4KII α (D308) mutant (Balla et al., 2002).

The dynamic aspects of intracellular trafficking molecules are not always amenable to study by immunofluorescence microscopy of fixed cells because the endosomal system of mammalian cells is composed of a number of morphologically heterogeneous membrane subcompartments (Maxfield and McGraw, 2004). Membrane markers are frequently trafficked throughout this pathway and, consequently, few antibodies exist which are able to unequivocally identify discrete endosomal compartments. Thus, although we find that PtdIns4KII α -containing structures can be readily distinguished

on the basis of their size and morphology in fixed cells (Fig. 1), we have also used the endocytosis of fluorescent EGF to study the role of PtdIns4KII α in receptor-mediated endocytosis. Not only did the use of Rh-EGF enable us to define early and late endosomal compartments by establishing a time course (Fig. 3), it also provided us with a well-characterised system in which, rather than being recycled, the ligand remains bound and is degraded along with the activated receptor (French et al., 1995). Thus trafficking of the EGF-EGFR complex through the endosomal system could be followed using Rh-EGF, providing an accurate readout for receptor endocytosis and for testing the function of PtdIns4KII α in this process.

The study of PtdIns4K function is hampered by a lack of specific small-molecule inhibitors, a situation compounded by the fact that overexpression of a kinase-inactive PtdIns4KII α (K152A) mutant failed to affect the endocytic traffic of Rh-EGF (data not shown). Other investigators have also noted that

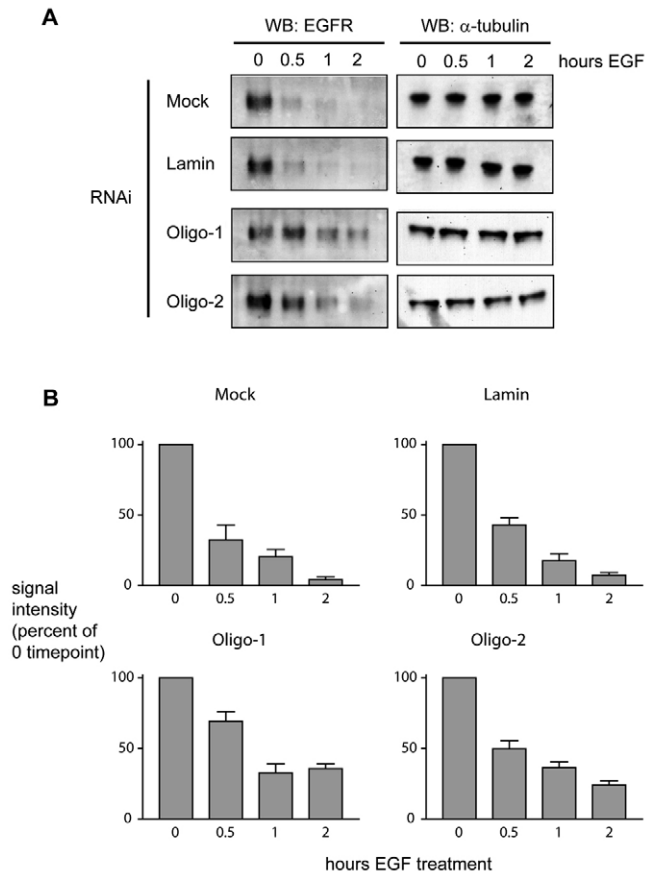


Fig. 8. Degradation of the EGF receptor is impaired in RNAi-treated HeLa cells. (A) Mock, lamin, oligo-1 or oligo-2 RNAi-transfected cells were treated with 100 ng/ml EGF for the times indicated in the presence of 10 μ g/ml cycloheximide and total cell lysates analysed by western blotting with anti-EGFR antibodies to monitor degradation of the EGFR and anti- α -tubulin antibodies to control for protein levels. (B) Densitometric analysis of western blot signals derived from three independent experiments (mean \pm s.e.m.).

kinase-inactive mutants do not substantially affect the localisation of PtdIns4KII α protein with endocytic markers (Balla et al., 2002). We therefore used several approaches to address PtdIns4KII α function: firstly we used the PtdIns4KII inhibitor PAO at 100 μ M. The fact that all traffic of GFP-PtdIns4KII α -containing vesicles ceased on addition of PAO is consistent with the idea that PtdIns4K activity is necessary for their transport. However, despite the widespread use of PAO as a PtdIns4K inhibitor, this compound is not expected to be specific (Balla et al., 2002; Yue et al., 2001). Consequently we looked to the inhibitory monoclonal antibody 4C5G. By introducing mAb 4C5G using the Chariot protein transfection system, we were able to monitor the effects of inhibition of endogenous PtdIns4KII on the endocytosis of Rh-EGF. This technique offered the advantage of a short incubation period (2 hours) and the acute inhibition of activity rather than PtdIns4KII protein synthesis as afforded by the use of RNAi. Finally we used siRNA to depress levels of endogenous PtdIns4KII α protein. Targeting of PtdIns4KII α in HeLa cells using RNAi has also been successfully used by others (Wang

et al., 2003). Transfection of HT1080 cells with siRNAs targeting PtdIns4KII α resulted in the isoform-specific inhibition of protein expression as judged by western blotting with PtdIns4KII α and PtdIns4KII β -specific antibodies (Fig. 6A). When HT1080 cells transfected with PtdIns4KII α siRNAs were treated with fluorescent EGF, internalisation initially appeared indistinguishable from that in mock-transfected cells. However, at time points greater than 120 seconds we observed several differences between siRNA-treated and mock-transfected control cells: firstly, internalised EGF accumulated in closely juxtaposed small vesicles in a sub-plasma membrane region, secondly, siRNA-treated cells had a reduced tendency to traffic EGF to juxtannuclear late endosomes, and thirdly, EGF internalised into smaller vesicles which were scattered throughout the cytoplasm rather than the juxtannuclear late endosomes observed in mock or lamin siRNA-transfected cells at similar time points (Fig. 6 and supplementary material Fig. S3). These results were entirely consistent with those observed on inhibition of endogenous PtdIns4KII activity by transfection with 4C5G which lead to dramatic changes in the organisation of internalised Rh-EGF compared with the control mAb 9E10. Indeed, all three characteristics of the RNAi experiment namely, sub-plasma membrane accumulation, inhibition of traffic to juxtannuclear late endosomes and scattered cytoplasmic early endosomes were observed with 4C5G.

These inhibition experiments provide independent evidence that PtdIns4KII α is a necessary factor in the endocytosis of EGF-EGFR complexes and that interference with PtdIns4KII α function results in a major perturbation of EGF endocytosis. The striking observation that EGF accumulates in endosomal vesicles clustered under the plasma membrane and scattered throughout the cytoplasm demonstrates a trafficking role for PtdIns4KII α – this is consistent with the observation that GFP-PtdIns4KII α and Rh-EGF colocalise in highly mobile vesicles (Figs 2 and 4).

A number of trafficking and sorting steps in the endosomal pathway are known to require PI lipids, in particular the 3'-phosphoinositides (for a review, see Gruenberg, 2003). Although trafficking roles have emerged for PtdIns(4) P in the Golgi (Godi et al., 2004), similar roles for PtdIns(4) P per se have not been described for the endo-lysosomal pathway. At present, we have been unable to detect significant amounts of PtdIns(4) P on transferrin, EEA1, lamp-1 or CD63-positive endosomes using either anti-PtdIns(4) P antibodies or by transfection with PtdIns(4) P -binding PH domains (data not shown). However this may simply be a technical issue reflecting the inability of the available probes to recognise endosomal PtdIns(4) P produced by PtdIns4KII α .

However PtdIns(4,5) P_2 , the product of the sequential action of PtdIns4K and PtdIns(4) P 5-kinase, is known to play important roles in receptor internalisation at the plasma membrane. For example, AP2, AP180 and epsin all bind PtdIns(4,5) P_2 and form part of the machinery that drives the formation of CCVs (Ford et al., 2002; Ford et al., 2001). PtdIns(4,5) P_2 is also required for the dynamin-dependent fission event that creates the endocytic vesicle destined for the early endosome (Marks et al., 2001). Thus it is possible that the effects of PtdIns4KII α inhibition observed in this study are due to the impairment of PtdIns(4,5) P_2 synthesis in one or more of these early steps. Indeed, the accumulation of small

vesicles clustered under the plasma membrane in PtdIns4KII α -inhibited cells would seem consistent with this suggestion. However, as inhibition of CCV formation efficiently prevents uptake of extracellular ligand (Ford et al., 2002), we favour the hypothesis that a later trafficking event is affected by PtdIns4KII α inhibition. Our data showing that Rh-EGF fails to properly traffic to juxtannuclear late endosomes demonstrates that an as yet undefined PtdIns(4)*P*-dependent trafficking step is impaired, which affects the traffic of early endosomal membranes to the late endosome, thus causing the accumulation of early endosomal and scattered cytoplasmic vesicles. Inhibition of this step ultimately impairs the degradation of the EGFR. Interestingly, endosomal carrier vesicles derived from early endosomal membranes are known to translocate to the late endosome on microtubules (Aniento et al., 1993) and the rate of movement of the rapidly moving vesicles observed in our time-lapse studies is characteristic of microtubule-mediated transport (Fig. 2 and supplementary material Movies 1 and 2). Indeed when GFP-PtdIns4KII α is photobleached in live HT1080 cells, recovery of late endosomal fluorescence can be inhibited by nocodazole treatment. (S.M., unpublished observations). Microtubule-dependent traffic to late endosomes involves the dynein-dynactin motor complex (Aniento et al., 1993). Intriguingly, in squid axons at least, this complex is dependent on acidic phospholipids and the PH-domain-containing molecule spectrin (Muresan et al., 2001). It is also notable that although PtdIns4KII α was found in late-endosomal membranes, we were unable to detect colocalisation with lysotracker (data not shown), suggesting that PtdIns4KII α is distributed between membranes of early and late but not lysosomal compartments.

Does PtdIns4KII α regulate the transfer of EGFR from early to late endosomal compartments? If this were the case we might expect the EGFR-containing vesicles in siRNA-treated cells to stain for early endosomal markers such as EEA1. However, we were unable to find an endosomal marker that quantitatively colocalised with the EGFR-containing scattered or sub-plasma membrane vesicles (data not shown). The identity of these structures and whether their persistence is responsible for the delay in EGFR degradation observed in siRNA-treated cells is currently under investigation in our laboratory.

While this manuscript was under review an independent study was published describing the association of PtdIns4KII α with AP-3-containing vesicles in PC12 cells (Salazar et al., 2005). Several aspects of their data are consistent with our study, firstly the authors report that endogenous PtdIns4KII α colocalises with lamp-1 by immunofluorescence, and secondly that AP-3 is delocalised by PtdIns4KII α RNAi. Since AP-3 function is linked to the traffic of proteins including hydrolytic enzymes to the lysosome, the affect of PtdIns4KII α knockdown on EGFR degradation seen here may be due to the inhibition of lysosomal enzyme traffic. In this regard it is interesting to note that the lysosomal membrane proteins lamp-1 and CD63 are delocalised in HT1080 cells transfected with siRNA targeting PtdIns4KII α (see supplementary material Fig. S4). Our data provide clear evidence for the necessity of PtdIns4KII α in receptor-mediated endocytosis and degradation and suggest a specific role in the traffic of endosomal carrier vesicles to the juxtannuclear late endosome. These results further broaden the scope of PtdIns4KII α function in

membrane traffic by placing them on highly dynamic endosomal membranes.

Materials and Methods

Antibodies, reagents and constructs

Human epidermal growth factor and all general reagents were obtained from Sigma (Poole, Dorset, UK). Polyclonal antisera to PtdIns4KII isoforms were raised as described (Vaughn et al., 2003a) and used here in western blotting. An additional anti-PtdIns4KII α rabbit polyclonal antiserum was raised to human recombinant PtdIns4KII α fused to the C-terminus of glutathione S-transferase. This antiserum was affinity-purified against the immunogen immobilised on glutathione-Sepharose beads and used for immunofluorescence microscopy (the isoform specificity of this antibody is demonstrated in supplementary material Fig. S1). Anti-lamp-1 and anti-EEA1 monoclonal antibodies were from BD Bioscience (Oxford, UK). Anti-GFP mAb was from Covance Research Products (Berkeley, CA). Anti-LBPA monoclonal antibody 6C4 was a kind gift from J. Gruenberg (Department of Biochemistry, University of Geneva, Switzerland). Anti-myc 9E10 monoclonal antibody was from Santa Cruz Biotechnology. Rabbit polyclonal anti-lamin A/C and anti-EGFR antibodies were from Cell Signaling Technology (New England Biolabs, Herts, UK). Monoclonal antibody 4C5G (Endemann et al., 1991) was as described (Minogue et al., 2001). Anti-CD63 monoclonal antibody 6H1 was as described (Berdichevski et al., 1995) Alexa Fluor 568 transferrin, human epidermal growth factor tetramethylrhodamine conjugate (Rh-EGF), monoclonal anti- α -tubulin, Alexa Fluor 488 goat anti-rabbit secondary conjugate and TetraSpeck fluorescent microspheres were all from Molecular Probes (Invitrogen, Paisley, UK). Human PtdIns4KII α cDNA (Minogue et al., 2001) was ligated into the pEGFP-C1 vector (BD Clontech, Oxford, UK) for expression as a green fluorescent protein (GFP) chimera. A K152A mutant was generated by site-directed mutagenesis using the QuikChange II mutagenesis system (Stratagene, La Jolla, CA) according to the manufacturer's instructions.

Cell culture and transfection

HT1080 fibrosarcoma cells stably expressing human recombinant GFP-PtdIns4KII isoforms were generated as follows: HT1080 cells were co-transfected with pEGFP-PtdIns4KII α or GFP-PtdIns4KII β (1 μ g each) and 0.2 μ g pZeoSV (Invitrogen) using FuGENE 6 (Roche Diagnostics, Lewes, UK). Two days after transfection, cells were split and re-plated in Dulbecco's modified Eagle's medium (DMEM) containing 100 μ g/ml Zeocin. Drug-resistant colonies (30-50) appeared in approximately 7-10 days. Cells expressing GFP-tagged constructs were subsequently selected in two rounds of cell sorting using a FACSVantage SE (BD Bioscience) equipped with CellQuest software.

For live-cell experiments, HT1080 cells expressing human recombinant GFP-PtdIns4KII α were seeded onto 35 mm glass-bottomed dishes and grown for 48 hours in Dulbecco's modified Eagle's medium containing 10% fetal bovine serum (FBS) at 37°C and 10% CO₂. Cells were similarly seeded and grown on glass coverslips prior to methanol fixation at -20°C for 3 minutes followed by immunostaining. When immunostaining with antibodies to EEA1, LBPA and PtdIns4KII α , cells were fixed in 4% paraformaldehyde for 5 minutes at room temperature and permeabilised in 0.05% saponin.

Scanning confocal microscopy

Microscopy was performed using an Axiovert 200M/LSM 510 Meta laser-scanning confocal microscope (Zeiss, UK). All images were obtained with a Zeiss Plan-Apochromat 63 \times 1.4 NA oil-immersion objective with pinholes set to one Airy unit. 12-bit fluorescence images were collected to peak by separate excitation of EGFP, Alexa Fluor 488, Alexa Fluor 568 and Rhodamine using the 488 nm and 543 nm lines produced by Kr/Ar (green) and He/Ne (red) lasers, respectively.

Live-cell studies were performed on the same instrument fitted with a heated stage insert (Zeiss, Herts, UK), on which HT1080 cells were maintained in HEPES-buffered medium at 37°C, 10% CO₂, and containing 10% FBS. Time-lapse images were captured in bidirectional scan mode in order to reduce scan times (not exceeding 1.19 seconds per frame). A similar imaging method was used for live HT1080-GFP-PI4KII α cells treated with Rh-EGF, except that EGFP and Rhodamine emissions were collected by separate excitation which increased the scan time to approximately 3 seconds per frame. For Rh-EGF stimulations, serum-starved cells were incubated with HEPES-buffered medium containing 100 ng/ml Rh-EGF for 30 seconds and the medium then replaced with fresh medium containing 100 ng/ml unlabelled EGF. Imaging (the zero time point) began within 120 seconds of Rh-EGF addition.

Data analysis and image handling

Images were exported from the LSM 510 software and were cropped and annotated in Adobe Photoshop 7.0. Unless otherwise stated, all images shown are single confocal sections. Microscopy data were analysed using Velocity 2.5 Classification (Improvision, Sheffield, UK) to obtain measurements of mean vesicle (object) diameter and rates of movement. In PtdIns4KII inhibition experiments, values for mean diameter of populations of Rh-EGF labelled punctae were obtained using Z-

series data from time course experiments and applying a classifier with thresholds for intensity and object size that were kept constant in all experiments. Objects below 0.05 μm in diameter or those touching each other were excluded from this analysis and measurements were routinely validated using 0.1–1.0 μm fluorescent Tetraspeck microspheres (Molecular Probes). Using randomly picked fields of view, at least three representative cells were analysed from each time point. Measurements generated between 300–800 objects per cell which were used to calculate the mean diameter for each population of vesicles. The data from at least three independent siRNA or 4C5G time course experiments were plotted using Prism 4.0 (GraphPad Software, San Diego, CA). In the case of the 4C5G inhibition experiments, insufficient fluorescent signals were obtained at the 120 second time point to accurately classify objects and so this time point does not appear in Fig. 7A. The same cells were manually scored for the presence of 'scattered' punctae and retention of small punctae at the plasma membrane. A minimum of 63 cells from randomly chosen fields were scored per time point. Criteria for scoring were as follows: any cell in which punctate Rh-EGF fluorescence was substantially non-perinuclear and cytoplasmic was judged as having scattered vesicles; any cell with punctate plasma membrane fluorescence was scored positive for retention of plasma membrane vesicles.

Protein transfection and RNA interference

Monoclonal antibody 4C5G was transfected into HT1080 cells using the chariot reagent (Active Motif, Rixensart, Belgium). This system is based on a short amphipathic peptide carrier (Morris et al., 2001) which, according to the manufacturer's data, is not internalised via the normal receptor-mediated endocytic pathway. Briefly, HT1080 cells were grown on coverslips for 24 hours and transfected with 1 μg 4C5G or 1 μg control mAb (9E10) for 2 hours according to the manufacturer's instructions. Cells were then serum-starved before pulse-chase stimulation with Rh-EGF as described above.

siRNA duplexes targeting human PtdIns4KII α (oligo-1, AAGCAGAACCUCU-CCUGAGA and oligo-2, GGACUUGGAAGAGCCUATT) were synthesized by Dharmacon RNA technologies (Lafayette, CO). SignalSilence siRNA specific for human lamin was obtained from Cell Signaling (NEB, UK). HT1080 cells were transfected once with 1.2 μM oligonucleotide for 96 hours using Oligofectamine (Invitrogen) according to the manufacturer's instructions. Specificity and degree of inhibition of PtdIns4KII expression was monitored by western blotting of total cell lysates with isotype-specific antisera to anti-PtdIns4KII α and anti-PtdIns4KII β (Vaugh et al., 2003a) as well as anti-Lamin A/C. HeLa cells were similarly transfected for EGFR degradation assays except that cells were grown in 35 mm dishes. Cell monolayers were serum-starved as described above and stimulated with unlabelled EGF for 0, 0.5, 1 and 2 hours in the presence of 10 $\mu\text{g}/\text{ml}$ cycloheximide in order to inhibit the de novo synthesis of EGFR. Total cell lysates were prepared and analysed by western blotting using a rabbit polyclonal anti-EGFR antibody (Cell Signaling) to monitor degradation of the 180 kDa EGFR band.

We are indebted to J. Gruenberg for kindly supplying mAb 6C4. We are grateful to Nick Beaumont and Claudia Wiedemann for their comments on the manuscript and Wendy Taylor for technical assistance. J.J.H. acknowledges the receipt of a Wellcome Trust Senior Fellowship. This work is additionally supported by the Wolfson Trust and the Peter Samuel Royal Free Fund.

References

Aniento, F., Emans, N., Griffiths, G. and Gruenberg, J. (1993). Cytoplasmic dynein-dependent vesicular transport from early to late endosomes. *J. Cell Biol.* **123**, 1373–1387.

Balla, A., Tuymetova, G., Barshishat, M., Geiszt, M. and Balla, T. (2002). Characterization of type II phosphatidylinositol 4-kinase isoforms reveals association of the enzymes with endosomal vesicular compartments. *J. Biol. Chem.* **277**, 20041–20050.

Berditchevski, F., Bazzoni, G. and Hemler, M. E. (1995). Specific association of CD63 with the VLA-3 and VLA-6 integrins. *J. Biol. Chem.* **270**, 17784–17790.

Cochet, C., Filhol, O., Payrastra, B., Hunter, T. and Gill, G. N. (1991). Interaction between the epidermal growth factor receptor and phosphoinositide kinases. *J. Biol. Chem.* **266**, 637–644.

Collins, C. A. and Wells, W. W. (1983). Identification of phosphatidylinositol kinase in rat liver lysosomal membranes. *J. Biol. Chem.* **258**, 2130–2134.

Cullen, P. J., Cozier, G. E., Banting, G. and Mellor, H. (2001). Modular phosphoinositide-binding domains – their role in signalling and membrane trafficking. *Curr. Biol.* **11**, R882–R893.

Endemann, G. C., Graziani, A. and Cantley, L. C. (1991). A monoclonal antibody distinguishes two types of phosphatidylinositol 4-kinase. *Biochem. J.* **273**, 63–66.

Felder, S., Miller, K., Moehren, G., Ullrich, A., Schlessinger, J. and Hopkins, C. R. (1990). Kinase activity controls the sorting of the epidermal growth factor receptor within the multivesicular body. *Cell* **61**, 623–634.

Ford, M. G., Pearce, B. M., Higgins, M. K., Vallis, Y., Owen, D. J., Gibson, A., Hopkins, C. R., Evans, P. R. and McMahon, H. T. (2001). Simultaneous binding of

PtdIns(4,5)P₂ and clathrin by AP180 in the nucleation of clathrin lattices on membranes. *Science* **291**, 1051–1055.

Ford, M. G., Mills, I. G., Peter, B. J., Vallis, Y., Praefcke, G. J., Evans, P. R. and McMahon, H. T. (2002). Curvature of clathrin-coated pits driven by epsin. *Nature* **419**, 361–366.

French, A. R., Tadaki, D. K., Niyogi, S. K. and Lauffenburger, D. A. (1995). Intracellular trafficking of epidermal growth factor family ligands is directly influenced by the pH sensitivity of the receptor/ligand interaction. *J. Biol. Chem.* **270**, 4334–4340.

Futter, C. E., Pearce, A., Hewlett, L. J. and Hopkins, C. R. (1996). Multivesicular endosomes containing internalized EGF-EGF receptor complexes mature and then fuse directly with lysosomes. *J. Cell Biol.* **132**, 1011–1023.

Godi, A., Pertile, P., Meyers, R., Marra, P., Di Tullio, G., Iurisci, C., Luini, A., Corda, D. and De Matteis, M. A. (1999). ARF mediates recruitment of PtdIns-4-OH kinase-beta and stimulates synthesis of PtdIns(4,5)P₂ on the Golgi complex. *Nat. Cell Biol.* **1**, 280–287.

Godi, A., Di Campli, A., Konstantakopoulos, A., Di Tullio, G., Alessi, D. R., Kular, G. S., Daniele, T., Marra, P., Lucoq, J. M. and De Matteis, M. A. (2004). FAPPs control Golgi-to-cell-surface membrane traffic by binding to ARF and PtdIns(4)P. *Nat. Cell Biol.* **6**, 393–404.

Gruenberg, J. (2003). Lipids in endocytic membrane transport and sorting. *Curr. Opin. Cell Biol.* **15**, 382–388.

Gruenberg, J. and Stenmark, H. (2004). The biogenesis of multivesicular endosomes. *Nat. Rev. Mol. Cell Biol.* **5**, 317–323.

Guo, J., Wenk, M. R., Pellegrini, L., Onofri, F., Benfenati, F. and De Camilli, P. (2003). Phosphatidylinositol 4-kinase type IIalpha is responsible for the phosphatidylinositol 4-kinase activity associated with synaptic vesicles. *Proc. Natl. Acad. Sci. USA* **100**, 3995–4000.

Hsuan, J. J. (1993). Oncogene regulation by growth factors. *Anticancer Res.* **13**, 2521–2532.

Katzmann, D. J., Odorizzi, G. and Emr, S. D. (2002). Receptor downregulation and multivesicular-body sorting. *Nat. Rev. Mol. Cell Biol.* **3**, 893–905.

Kauffmann-Zeh, A., Klinger, R., Endemann, G., Waterfield, M. D., Wetzker, R. and Hsuan, J. J. (1994). Regulation of human type II phosphatidylinositol kinase activity by epidermal growth factor-dependent phosphorylation and receptor association. *J. Biol. Chem.* **269**, 31243–31251.

Kobayashi, T., Stang, E., Fang, K. S., de Moerloose, P., Parton, R. G. and Gruenberg, J. (1998). A lipid associated with the antiphospholipid syndrome regulates endosome structure and function. *Nature* **392**, 193–197.

Marks, B., Stowell, M. H., Vallis, Y., Mills, I. G., Gibson, A., Hopkins, C. R. and McMahon, H. T. (2001). GTPase activity of dynamin and resulting conformation change are essential for endocytosis. *Nature* **410**, 231–235.

Maxfield, F. R. and McGraw, T. E. (2004). Endocytic recycling. *Nat. Rev. Mol. Cell Biol.* **5**, 121–132.

Minogue, S., Anderson, J. S., Waugh, M. G., dos Santos, M., Corless, S., Cramer, R. and Hsuan, J. J. (2001). Cloning of a human type II phosphatidylinositol 4-kinase reveals a novel lipid kinase family. *J. Biol. Chem.* **276**, 16635–16640.

Morris, M. C., Depollier, J., Mery, J., Heitz, F. and Divita, G. (2001). A peptide carrier for the delivery of biologically active proteins into mammalian cells. *Nat. Biotechnol.* **19**, 1173–1176.

Muresan, V., Stankewich, M. C., Steffen, W., Morrow, J. S., Holzbaur, E. L. and Schnapp, B. J. (2001). Dynactin-dependent, dynein-driven vesicle transport in the absence of membrane proteins: a role for spectrin and acidic phospholipids. *Mol. Cell* **7**, 173–183.

Oh, P., McIntosh, D. P. and Schnitzer, J. E. (1998). Dynamin at the neck of caveolae mediates their budding to form transport vesicles by GTP-driven fission from the plasma membrane of endothelium. *J. Cell Biol.* **141**, 101–114.

Roskoski, R., Jr (2004). The ErbB/HER receptor protein-tyrosine kinases and cancer. *Biochem. Biophys. Res. Commun.* **319**, 1–11.

Salazar, G., Craig, B., Wainer, B. H., Guo, J., De Camilli, P. and Faundez, V. (2005). Phosphatidylinositol-4-kinase type II alpha is a component of adaptor protein-3-derived vesicles. *Mol. Biol. Cell* **16**, 3692–3704.

Wang, Y. J., Wang, J., Sun, H. Q., Martinez, M., Sun, Y. X., Macia, E., Kirchhausen, T., Albanesi, J. P., Roth, M. G. and Yin, H. L. (2003). Phosphatidylinositol 4 phosphate regulates targeting of clathrin adaptor AP-1 complexes to the Golgi. *Cell* **114**, 299–310.

Waugh, M. G., Minogue, S., Anderson, J. S., Balinger, A., Blumenkrantz, D., Calnan, D. P., Cramer, R. and Hsuan, J. J. (2003a). Localization of a highly active pool of type II phosphatidylinositol 4-kinase in a p97/valosin-containing-protein-rich fraction of the endoplasmic reticulum. *Biochem. J.* **373**, 57–63.

Waugh, M. G., Minogue, S., Blumenkrantz, D., Anderson, J. S. and Hsuan, J. J. (2003b). Identification and characterization of differentially active pools of type II phosphatidylinositol 4-kinase activity in unstimulated A431 cells. *Biochem. J.* **376**, 497–503.

Wei, Y. J., Sun, H. Q., Yamamoto, M., Wlodarski, P., Kunii, K., Martinez, M., Barylko, B., Albanesi, J. P. and Yin, H. L. (2002). Type II phosphatidylinositol 4-kinase beta is a cytosolic and peripheral membrane protein that is recruited to the plasma membrane and activated by Rac-GTP. *J. Biol. Chem.* **277**, 46586–46593.

Wiedemann, C., Schafer, T. and Burger, M. M. (1996). Chromaffin granule-associated phosphatidylinositol 4-kinase activity is required for stimulated secretion. *EMBO J.* **15**, 2094–2101.

Yue, J., Liu, J. and Shen, X. (2001). Inhibition of phosphatidylinositol 4-kinase results in a significant reduced respiratory burst in formyl-methionyl-leucyl-phenylalanine-stimulated human neutrophils. *J. Biol. Chem.* **276**, 49093–49099.